OFFICE OF NAVAL RESEARCH

Contract N00014-89-J-1530

Task No. NR372-160

TECHNICAL REPORT NO. 30

FINITE DEBYE-WALLER FACTOR FOR "CLASSICAL" ATOM-SURFACE SCATTERING

by

K. Burke and W. Kohn

Prepared for publication

in

Phys. Rev. B (1990)

Department of Physics

University of California, Santa Barbara

Santa Barbara, CA 93106

August 1990

SECURITY CLASSIFICATION OF THIS PAGE (When Data Entered)

REPORT DOCUMENTATION PAGE

READ INSTRUCTIONS BEFORE COMPLETING FORM

1. REPORT NUMBER: TECHNICAL REPORT NO. 30	2. GOVT ACCESSION NO.
3. RECIPIENT'S CATALOG NUMBER: N00014-01	
4. TITLE (and Subtitle): FINITE DEBYE-WALLER FACTOR FOR "CLASSICAL" ATOM-SURFACE SCATTERING	5. TYPE OF REPORT & PERIOD COVERED: TECHNICAL REPORT 1/01/90--12/31/90
	6. PERFORMING ORG. REPORT NUMBER
7. AUTHOR(s): K. BURKE AND W. KOHN	8. CONTRACT OR GRANT NUMBER(s): N00014-89-J-1530
9. PERFORMING ORGANIZATION NAME AND ADDRESS: UNIVERSITY OF CALIFORNIA PHYSICS DEPARTMENT, SANTA BARBARA, CA 93106 CONTRACTS & GRANTS, CHEADLE HALL, ROOM 3227	10. PROGRAM ELEMENT, PROJECT, TASK AREA & WORK UNIT NUMBERS: TASK NO. 372-160
11. CONTROLLING OFFICE NAME AND ADDRESS: OFFICE OF NAVAL RESEARCH ELECTRONICS & SOLID STATE PHYSICS PROGRAM 800 N. QUINCY, ARLINGTON, VA 22217	12. REPORT DATE: 8/90 13. NUMBER OF PAGES: -2-
14. MONITORING AGENCY NAME & ADDRESS (if different from Controlling Office): OFFICE OF NAVAL RESEARCH DETACHMENT 1030 EAST GREEN STREET PASADENA, CA 91106	15. SECURITY CLASS. (of this report): UNCLASSIFIED 15a. DECLASSIFICATION/DOWNGRADING SCHEDULE

16. DISTRIBUTION STATEMENT (of this Report)

"APPROVED FOR PUBLIC RELEASE: DISTRIBUTION UNLIMITED"

17. DISTRIBUTION STATEMENT (of the abstract entered in Block 20, if different from Report)

REPORTS DISTRIBUTION LIST FOR ONR
PHYSICS DIVISION OFFICE--

18. SUPPLEMENTARY NOTES

Phys. Rev. B (1990)

19. KEY WORDS (Continue on reverse side if necessary and identify by block number)

quantum mechanical scattering, classical scattering, quasi-adiabatic regime, Debye-Waller Factor, adiabatic collision variables, atom-surface interaction, trajectory approximation

20. ABSTRACT (Continue on reverse side if necessary and identify by block number)

We consider atom-surface scattering at low surface temperature, fixed incident energy and fixed interaction potential. We examine the limit as the mass m of the incident particle $\to\infty$, and thus its de Broglie wavelength $\to 0$. We show that in this "classical" limit, the Debye-Waller factor (a quantum effect) for the strictly elastic scattering amplitude tends to a finite limit. We propose scattering of 20 meV Ar atoms from cold Cu(111) as a promising experiment to verify this effect.

DD FORM 1 JAN 73 1473 EDITION OF 1 NOV 65 IS OBSOLETE

S/N 0102-LF-014-6601

SECURITY CLASSIFICATION OF THIS PAGE (When Data Entered)

Finite Debye-Waller Factor for "Classical" Atom-Surface Scattering

(Final Version: May 31, 1990)

K. Burke* and W. Kohn

Department of Physics

University of California

Santa Barbara, CA 93106

Abstract: We consider atom-surface scattering at low surface temperature, fixed incident energy and fixed interaction potential. We examine the limit as the mass m of the incident particle $\rightarrow \infty$, and thus its de Broglie wavelength $\rightarrow 0$. We show that in this "classical" limit, the Debye-Waller factor (a quantum effect) for the strictly elastic scattering amplitude tends to a finite limit. We propose scattering of 20 meV Ar atoms from cold Cu(111) as a promising experiment to verify this effect.

I. Introduction

Surface scattering experiments are generally regarded from the standpoints of two extreme regimes: the quantum mechanical regime or the classical regime. Consider a surface which is cold ($T \approx 0$) and relatively smooth (exhibits little or no diffraction). Then quantum mechanical scattering is exemplified by a light incident atom such as He with a low initial energy of say, 20 meV. Under these conditions, one-phonon peaks may be easily distinguished, and the technique is often used to measure surface phonon dispersion curves.[1] On the other hand, classical scattering occurs with heavy incident particles such as Xe at hyperthermal energies[2] of several eV. The results of such experiments are usually compared to either classical or semiclassical calculations.[3] The transition between these two regimes is continuous. However, it is generally expected[4] that, as the mass of the incident atom is increased, characteristic quantum effects disappear. We will however show that (in a particular sense) quantum effects remain finite, if the initial energy of the incident atom is kept fixed.

To clarify the discussion, we re-express the distinction of regimes in terms of the following dimensionless parameters : λ/d and $\bar{n}$, where λ is the de Broglie wavelength of the incident atom, d is a "range" of the atom surface interaction, and $\bar{n}$ is the mean number of phonons excited by the collision. Consider first scattering from a rigid lattice. Then the incident atom behaves classically if $\lambda \ll d$ and quantum mechanically if $\lambda \gtrsim d$. Similarily, the lattice behaviour is characterized by $\bar{n}$. If after the collision $\bar{n} \sim O(1)$, the lattice exhibits quantum effects, while for $\bar{n} \gg 1$, it behaves classically. For the experiments described above, both incident atom and lattice behave either classically or quantum mechanically. A typical energy loss spectrum in the latter regime, integrated over all outgoing directions, is shown in Fig. 1. At $\Delta E = 0$, there is a substantial no-loss line due to elastic scattering from the surface (this has been broadened in the figure to simulate a finite en-

ergy resolution). This is a characteristic quantum effect since, for classical scattering with a finite incident energy, there is necessarily a finite energy loss to the lattice.[5] We refer to the scattering as weakly inelastic when most of the outgoing distribution lies in the no-loss line.

In this paper, we are interested in a mixed regime : $\lambda \ll d$ but $\bar{n} \sim O(1)$. This may be achieved physically by a heavy particle (of mass m) with low incident energy E striking a surface. For fixed E, as m is increased, the initial velocity of the incident atom v decreases and the scattering becomes increasingly adiabatic and more and more nearly elastic. In the limit of infinite mass, the scattering is completely elastic, and the adiabatic limit is achieved. For large but *finite* m, the scattering is almost adiabatic, and we call this the quasi-adiabatic regime. In this regime, the energy loss spectrum of Fig. 1 is compressed toward the $\Delta E = 0$ region. However, assuming we have sufficient energy resolution to determine its shape, there are three possibilities which may be imagined : (1) the scattering becomes completely elastic and the inelastic shoulder disappears, (2) the system behaves classically, and the elastic no-loss line disappears or (3) a finite fraction of both elastic and inelastic scattering remain, as illustrated in Fig. 2. We show in this work that the third of these possibilities actually occurs, providing a striking demonstration of a quantum mechanical effect that does not vanish as the mass of the incident atom grows large. (However, the splitting between the elastic peak and the inelastic shoulder approaches zero.)

In section II of this paper, we make a realistic estimate of the Debye-Waller factor in the limit of large m, but first we give a simple plausibility argument for the above claims. Let us denote by v the velocity of the particle during the interaction, and by $\tau(\equiv d/v)$ the nominal collision time. As m grows, τ grows as $m^{1/2}$. The slowly varying force exerted by the incident atom on the surface atoms can excite only those modes with frequencies $\omega \lesssim 1/\tau$, i.e. only long wavelength acoustic phonons. The probability of exciting a single

phonon of frequency ω is then approximately[6]

$$P^{(1)}(\omega) \sim \Delta k_3^2 u_3^2(\omega), \tag{1}$$

where Δk_3 is the perpendicular momentum transfer to the surface for elastic scattering and $u_3^2(\omega)$ is the contribution from a normal mode of frequency ω to the mean square vibration of a surface atom perpendicular to the surface in the undisturbed crystal. The elastic fraction, written e^{-2W}, is the Debye-Waller factor . For small W, $e^{-2W} \approx 1 - 2W$ and by flux conservation

$$2W \sim \sum_{\omega \lesssim 1/\tau} \Delta k_3^2 u_3^2(\omega). \tag{2}$$

This is just the standard expression for the Debye-Waller factor (well known from X-ray and neutron scattering [7]), except for the cut-off at $\omega \approx 1/\tau$ due to the slowness of the incident atom. We may estimate $2W$ using the bulk properties of the solid in the Debye model:[8]

$$2W \sim \frac{(2k_3)^2}{\omega_D^3} \int_0^{1/\tau} \left(\frac{\hbar}{2M\omega}\right) \omega^2 d\omega \sim \left(\frac{E_\perp}{\hbar\omega_D}\right)^2 \frac{\langle u_3^2 \rangle}{d^2}, \tag{3}$$

where ω_D is the Debeye frequency of the crystal, M the mass of a lattice atom, $E_\perp \equiv k_3^2/2m$, and $< u_3^2 >$ is the mean square of zero point vibrations in the crystal perpendicular to the surface. Note that this is independent of m, and therefore W remains finite as $m \to \infty$. Finally we note that, with an attractive well of depth D, $E_\perp$ should be replaced by $E_\perp + D$ in equation (3) (the Beeby correction).[9] Thus, we still find a finite Debye-Waller factor for $m \to \infty$.

In section II we describe our model for the atom-surface interaction and the approximations used to calculate W more accurately. The quasi-adiabatic regime is discussed and illustrated in section III by simple models for the interaction. In section IV, we apply these results to noble gas scattering from metal surfaces, and suggest an experiment for the case of Ar scattering from Cu(111). We choose this system because the static corrugation is

expected to be small (so that diffraction effects may be neglected) and because it provides an experimentally accessible system with a relatively heavy incident atom. Properties of other systems are compared with this. In section V we discuss our results and their implications for future work, both theoretical and experimental. Appendices A and B deal with technical details; appendix C demonstrates the validity of the trajectory approximation for weakly inelastic scattering in the quasi-adiabatic regime.

II. Theoretical Formulation

In this section, we introduce a model for the atom-surface interaction and demonstrate how the final energy and angular distributions may be calculated from it. We are interested in the quasi-adiabatic regime, achieved by $m \to \infty$, keeping E and all substrate properties fixed. However, to simplify the calculations, we make several approximations which are valid for noble gases scattering from metal surfaces at thermal energies, the specific systems studied in this paper. For example, we assume throughout that the displacements of the surface atoms are small. We also use the trajectory approximation [10] (TA) to calculate the scattered distribution. Although the validity of the TA is proved here (Appendix C) only for weakly inelastic ,quasi-adiabatic scattering , we expect that the qualitative conclusions remain valid also for strongly inelastic scattering. Throughout, we use the standard notation for surface scattering : A vector v has components V in the surface plane and v_3 perpendicular to it; its length is denoted by v. The only exception to this is the use of z to denote the component of the incident atom's position perpendicular to the surface. We also use, in general, primed letters to denote quantities after the collision.

A. The Atom-Surface Interaction

We make the Born-Oppenheimer approximation[11] for the electronic motion, which is

valid in this regime. Then a general atom-surface interaction may be written $V(\mathbf{r},\{\mathbf{u}\})$ where $\mathbf{r}$ is the position of the incident atom, and the set $\{\mathbf{u}\}$ is the set of all displacements of the atoms from their equilibrium positions in the crystal lattice. We make the assumption (for simplicity only) that it may be modeled by a "perpendicular" potential function of the form

$$V(\mathbf{r},\{\mathbf{u}\}) \simeq V_{\perp}(z - Z(\mathbf{R},\{\mathbf{u}\})), \tag{4}$$

where $\mathbf{r} = (\mathbf{R}, z)$ is the position of the incident atom and $Z(\mathbf{R},\{\mathbf{u}\})$ is the so called corrugation function for the atom-surface system, which is chosen to best model the true many-body potential. The corrugation function will also be a function of incident energy, not written explicitly here. For the small incident energies discussed here, the incident atom remains far from the surface atoms, and this approximation will be valid. For small displacements of the surface atoms,

$$V(\mathbf{r},\{\mathbf{u}\}) = V(\mathbf{r},\{0\}) + \sum_{\mathbf{l}} \mathbf{u}_{\mathbf{l}}.\nabla_{\mathbf{l}} V\Big|_{\mathbf{r},\{0\}} + \ldots, \tag{5}$$

where $\mathbf{l}$ labels each equilibrium site in the crystal, and $\{0\}$ indicates no displacements from equilibrium; the gradient with respect to $\mathbf{u}_{\mathbf{l}}$ is denoted $\nabla_{\mathbf{l}}$. Then, for a perpendicular potential, as defined by equation (4),

$$V(\mathbf{r},\{\mathbf{u}\}) = V_{\perp}(z - Z_0(\mathbf{R})) - \sum_{\mathbf{L}} \mathbf{u}_{\mathbf{L}}.\mathbf{f}(\mathbf{R}-\mathbf{L}) \frac{\partial V_{\perp}}{\partial z}\Big|_{z - Z_0(\mathbf{R})} + \ldots, \tag{6}$$

where $Z_0(\mathbf{R})(\equiv Z(\mathbf{r},\{\mathbf{0}\}))$ is the static corrugation of the surface, and $\mathbf{f}(\mathbf{R})$ is the so-called transfer function, defined by

$$\mathbf{f}(\mathbf{R}) = \frac{\partial Z(\mathbf{R},\{\mathbf{u}\})}{\partial \mathbf{u_0}}\Big|_{\mathbf{R},\{0\}}. \tag{7}$$

An illustration of $Z_0(\mathbf{R})$ and $\mathbf{f}(\mathbf{R})$ is given in Fig. 3. For short-range interactions, displacements of atoms beneath the surface will have small effects on the potential seen by the incident atom so we retain only the $l_3 = 0$ (surface layer) term in the sum in equation

(6). From equation (6) we see that this function, coupled with knowledge of the elastic scattering potential, $V_\perp(z - Z_0(\mathbf{R}))$, and its first derivative, is sufficient to determine the potential for small displacements of surface atoms. Then, for a system of negligible static corrugation, the Hamiltonian takes the form

$$H = H_{inc} + H_0 + F_\perp(z).\xi(\mathbf{R}), \tag{8}$$

where $H_{inc} = p^2/2m + V_\perp(z)$ is just the Hamiltonian for the incident particle scattering from a rigid latttice, H_0 is the Hamiltonian for the undisturbed crystal, $F_\perp(z) = -\partial V_\perp(z)/\partial z$ is the force exerted on the incident atom by the crystal and $\xi(\mathbf{R}) = \sum \mathbf{u_L}.\mathbf{f}(\mathbf{R} - \mathbf{L})$ is linear in the surface atomic displacements. We expand the displacements in terms of the harmonic normal modes of the half-crystal:

$$\mathbf{u_L} = \sum_q u(\omega_q)\mathbf{v}_q(a_q + a^\dagger_{-q})e^{i\mathbf{Q}.\mathbf{L}}, \tag{9}$$

where

$$u(\omega_q) = \frac{\hbar}{\sqrt{2NM\omega_q}}. \tag{10}$$

In this expression, advantage has been taken of the translational symmetry parallel to the surface ; N is the number of atoms in the crystal; M is the mass of a crystal atom; $\mathbf{Q}$ is the phonon momentum parallel to the surface; $q = \{\mathbf{Q}, q_3\}$ labels the $3N$ different modes and $-q = \{-\mathbf{Q}, -q_3\}$; $a^\dagger_q$ and a_q are creation and annhilation operators for phonons labelled q, with frequency ω_q and displacement vector $\mathbf{v}_q$ in the surface layer. The function $u(\omega_q)$ is just the magnitude of the zero point displacement in the bulk due to a bulk phonon of frequency ω_q, while surface effects are contained in the displacement vector $\mathbf{v}_q$. Its normalization and dependence on ω_q are given in appendix B. We also define the surface Fourier transform of the transfer function

$$\tilde{\mathbf{f}}(\mathbf{K}) \equiv \frac{1}{\mathcal{A}}\int_S d^2\mathrm{R}e^{i\mathbf{K}.\mathbf{R}}\mathbf{f}(\mathbf{R}), \tag{11}$$

where $\mathcal{A}$ is the area of the surface unit cell, and $\mathcal{S}$ represents the entire surface. The sum over $\mathbf{L}$ now yields

$$\xi(\mathbf{R}) = \sum_{\mathbf{G},q} \tilde{\mathbf{f}}(\mathbf{G}+\mathbf{Q}) \cdot \mathbf{v}_q e^{i\mathbf{Q}\cdot\mathbf{R}} u(\omega_q)(a_q + a^\dagger_{-q}). \tag{12}$$

As only low frequency modes are excited, we approximate $\tilde{\mathbf{f}}(\mathbf{K})$ by its behaviour in the long wavelength limit which yields

$$\xi(\mathbf{R}) = \sum_{q} (\mathbf{v}_q)_3 e^{i\mathbf{Q}\cdot\mathbf{R}} u(\omega_q)(a_q + a^\dagger_{-q}) \tag{13}$$

(see appendix A).

B. The Trajectory Approximation

Although the Hamiltonian has been simplified by the approximations of section A, the scattering problem is still not easily solved, especially for strongly inelastic scattering. We therefore solve it within the trajectory approximation (TA),[10] in which the incident particle is treated classically, while the surface is treated quantum mechanically. For weakly inelastic scattering in the quasi-adiabatic regime, this is shown to be valid in appendix C.

First we calculate the classical trajectory of the incident atom, with the atoms fixed in their equilibrium positions. This is the so-called recoilless classical trajectory. We then have a simple classical one-dimensional scattering problem with a potential of the form shown in Fig. 4. For this uniform potential, the classical equations of motion decouple, and we write

$$\mathbf{r} = (\mathbf{V}t, z_{cl}(t)) \tag{14}$$

where $\mathbf{V}$ is the initial velocity parallel to the surface . The TA Hamiltonian then becomes (see equations (8) and (13))

$$H_{TA} = \sum_q \omega_q (a_q a_q^\dagger + 1/2) + \sum_q U_q(t)(a_q + a^\dagger_{-q}), \tag{15}$$

where

$$U_q(t) = F(t)e^{i\mathbf{Q}.\mathbf{V}t}u(\omega_q)(\mathbf{v}_q)_3. \tag{16}$$

The function $F(t)$ is just $F_\perp(z)$ evaluated on the classical trajectory $z_{cl}(t)$. This Hamiltonian describes a set of uncoupled linearly driven oscillators, whose final states and corresponding energy and momentum changes may be easily calculated.[10] The distribution of energy loss and momentum exchange of the incident atom is then deduced from conservation laws to be

$$\mathcal{N}(\Delta E, \Delta\mathbf{K}) = \int dt \int d^2\mathbf{R}\mathcal{N}(t,\mathbf{R})e^{i\Delta Et + i\Delta\mathbf{K}.\mathbf{R}} \tag{17}$$

where

$$\mathcal{N}(t,\mathbf{R}) = \exp\Big\{\sum_q |U_q(\omega_q)|^2(\exp[-i\omega_q t - i\mathbf{Q}.\mathbf{R}] - 1) \tag{18}$$

The variables ΔE and $\Delta\mathbf{K}$ denote the energy loss and surface momentum exchange respectively, while $U_q(\omega)$ is the Fourier transform of $U_q(t)$. The constant term (independent of t and $\mathbf{R}$) *in equation* (18) *gives* a contribution to the final spectrum proportional to $\delta(\Delta E)\delta(\Delta\mathbf{K})$, i.e. it is the Debye-Waller factor . Using equation (16) it can be written as

$$2W = \sum_q F^2(\omega_q + \mathbf{Q}.\mathbf{V})u^2(\omega_q)|(\mathbf{v}_q)_3|^2. \tag{19}$$

This result has the same form as equation (3), as $F(0) = \Delta k_3$ and for large incident mass $F(\omega_q)$ will be cut-off at about $1/\tau$. In the next section we will analyze this result and the energy loss spectrum in the quasi-adiabatic regime in more detail.

III. The Quasi-Adiabatic Regime

In this section we discuss the behaviour of the energy and momentum transfer distribution found in section II (equation (18)) in the quasi-adiabatic regime. We introduce dimensionless variables to show explicitly the dependence on m of each quantity calculated.

In particular, we find that the mean number of phonons excited and the Debye-Waller factor are independent of m, while other properties, such as the shape of the energy loss distribution, scale in simple ways with m.

To begin with, we restrict our attention to normal incidence on a surface at zero temperature, and calculate the angle-integrated energy loss spectrum. For the classical trajectory of the incident atom, we choose the origin in space and time to be at the position and moment of turning , i.e. $dz/dt = 0$ at $z = 0$ and $t = 0$. As we are interested in the behaviour of the system as $m \to \infty$ we write the trajectory in terms of the dimensionless variables used in section I : $\zeta = z/d$, $s = t/\tau$ and[12] $\phi(\zeta) = V_\perp(z)/E$. The equation of motion for ζ is then

$$\zeta'' = -\frac{d\phi}{d\zeta}, \tag{20}$$

where $\zeta'' \equiv d^2\zeta/ds^2$. The boundary conditions are $\zeta'(\pm\infty) = \pm 1$. With this choice of origin, $\zeta(s)$ is symmetric in s, and independent of m (but not of E). In terms of these variables, the energy loss spectrum is denoted $\mathcal{N}_\epsilon$, where $\epsilon = \Delta E\tau/\hbar$ and the normalization is chosen so that $\int \mathcal{N}_\epsilon d\epsilon/2\pi = 1$. Then, from equation (16), with $\mathbf{R} = \mathbf{0}$, we may write its Fourier transform as

$$\mathcal{N}(s) = \exp\{\alpha[\chi(s) - \chi(0)]\}, \tag{21}$$

where

$$\chi(s) = \int_0^\infty d\nu |\zeta''_\nu|^2 \nu e^{-i\nu s}, \tag{22}$$

$$\alpha = 24\left(\frac{E}{\hbar\omega_D}\right)^2 \frac{< u_3^2 >_s}{d^2}, \tag{23}$$

and ζ''_ν is the Fourier transform of $\zeta''(s)$. In these expressions, we use the long wavelength limit to calculate the phonon properties, as described in appendix B. The quantity $< u_3^2 >_s$ is a measure of the zero point displacements perpendicular to the surface of atoms in the surface, and is also described in appendix B. The Debye-Waller factor is then given by

$\exp -\alpha\chi(0)$, so that[13]

$$2W = \alpha I_1, \tag{24}$$

where $I_n = \int_0^\infty d\nu \nu^n |\zeta''_\nu|^2$. This shows explicitly that $2W$ is independent of m, and has the form of equation (3).

To illustrate these results we use two simple potentials for which analytic results may be obtained : the exponential repulsion and the Morse potential. For both potentials we choose d to be the decay length of the repulsive part of the potential and $\alpha = 0.1$, a value appropriate for the experimental conditions discussed in section IV. For the Morse potential, we also choose a well-depth $D = 2.3E$ for the same reason. The dimensionless forms for the Fourier transform of the acceleration are then

$$\zeta''_\nu = \frac{2\pi\nu}{\sinh\pi\nu} \tag{25}$$

for the pure exponential repulsion and

$$\zeta''_\nu = \frac{2\pi\nu}{\sinh\pi\nu}\frac{\cosh\beta\pi\nu}{\cosh\pi\nu} \tag{26}$$

for the Morse potential. Here β is a function of E/D, with a value of 1.6 for our case.[14] These functions are plotted in Fig. 4, and their corresponding final energy spectra in Fig. 5. The dramatic difference is due to the attractive well, which accelerates the incident particle as it passes over it. From Table I, we see that this greatly enhances I_1, leading to a major decrease in the Debye-Waller factor. We stress the fact that this reduction is entirely due to the attractive well, and is not due to the large incident mass.

To clarify further our discussion of the loss spectrum, we introduce a number of parameters characteristic of the collision. From the spectrum given by equation (18), it can be shown that the mean phonon frequency to which the incident atom couples is $\bar{\omega} = (I_2/I_1)\tau^{-1}$. The mean energy loss may also be calculated, and we find $\overline{\Delta E} = \hbar\alpha I_2/\tau$. Then a measure of the number of phonons excited during the collision is given by $\bar{n} =$

$\overline{\Delta E}/\bar{\omega}$, or

$$\bar{n} = 2W. \tag{27}$$

The meaning of this result is intuitively clear : when few phonons are excited ($\bar{n} \ll 1$), the scattering is predominantly elastic (weakly inelastic scattering), while for $\bar{n} \gg 1$, the converse is true.

Next, we briefly discuss temperature effects. Equation (18) may be easily generalized[10] to finite surface temperature, T. The only change this leads to in equation (19) is an extra multiplicative factor of $\coth(\omega_q/2k_BT)$, due to the thermal motion of the crystal atoms. For small T, the Debye-Waller factor behaves as a gaussian function of T. We find $W(T) = W(0) + T^2/\bar{T}^2$, with

$$\bar{T} = \frac{T_\tau}{2\pi}\sqrt{\frac{3}{8\alpha}} \tag{28}$$

where $k_BT_\tau = \hbar/\tau$. From the definition of α (equation (24)) and using $\tau = d/v$, it is straightforward to show that $\bar{T}$ is independent of the functional form of the potential. However, the range of temperature over which the Debye-Waller factor displays gaussian behaviour *is* determined by the form of the interaction potential. For high temperatures ($T \gg T_\tau$) the usual exponential dependence of the Debye-Waller factor is regained, with a decay temperature of

$$\bar{T} = \frac{T_\tau}{2\alpha I_0}. \tag{29}$$

The dependence of $\bar{T}$ on the other parameters differs markedly from standard expressions,[6] due to the cutoff in $F_\perp(\omega)$ at $1/\tau$.

For any finite temperature, as long as m is finite, there is a finite Debye-Waller factor . However, as $m \to \infty$ with T finite, $T \gg T_\tau$, so that $\coth(\omega_q/2k_BT) \gg 1$ for all excited phonons, and the probability of excitation is greatly enhanced. Hence, as $m \to \infty$, the Debye-Waller factor approaches zero.

The angular distribution is gaussian, of width

$$\theta_W = \sqrt{\frac{8\alpha I_3 \mu}{3}}\left(\frac{v_a}{c_t}\right) \tag{30}$$

where $v_a = \hbar/md$ and c_t is the transverse speed of sound in the crystal. The dimensionless constant μ is an elastic property of the crystal, with a value of 0.9 for Cu (Appendix B).

IV. Application to Scattering of Rare Gases

We begin our discussion of results with the system : Ar incident on Cu(111) with an initial energy of 20 meV. This is a good system for experimental verification of this effect for a number of reasons. Of primary importance is the fact that Ar is sufficiently heavy, so that the quasi-adiabatic regime may be achieved at low incident energy. Furthermore, the well-depth of the interaction potential is sufficiently small so that the elastic peak remains resonably strong (see Fig. 4). Another useful feature which simplifies the calculation is the smoothness of a (111) metal surface, which allows us to neglect diffraction. However, even with these simplifications, we offer only a semiquantitative calculation of the Debye-Waller factor . Our purpose is simply to show that this effect occurs for Ar scattering from Cu, and that it is detectable.

For the elastic scattering potential we assume a simple exponential repulsion plus a long range Van der Waals attraction:

$$V_0(z) = A_0 e^{-z/d} - \frac{C_3}{(z - z_{ref})^3} \tag{31}$$

The constants C_3 and z_{ref} are given by Zaremba and Kohn.[15] We expect the Ar - Cu repulsion to have approximately the same z-dependence as the He - Cu repulsion (as suggested by the Norskov recipe)[16]. The proportionality constant[17] is 4.6. We also take the He - Cu repulsion from Zaremba and Kohn.[15] The values we use are listed in Table II, along with other characteristics of the potential. These numbers are only estimates,

and should not be regarded as highly accurate. The most important characteristics of the potential are the decay length of the repulsion and the well-depth, which is 45 meV. For our purposes, its properties are very similar to that of a Morse potential of equal depth and decay length, the difference in the long-range attraction being of no importance.

The energy loss spectrum, integrated over all outgoing directions, calculated in the TA, is plotted in Fig. 5. The surface is at zero temperature. The spectrum has been convoluted with a gaussian of width 2 meV, to simulate an experimental resolution of 10%. Its shape is very similar to that of the Morse potential shown in Fig. 4, except for the cutoff at the incident energy. The elastic peak contains about 10% of the scattered particles, while another 50% are scattered into the inelastic shoulder. A further 40% remain stuck to the surface (negative final energy in the trajectory approximation). The energy of the incident particles in the interaction well is $\approx$ 65 meV, whereas the calculated mean energy of the scattered particles is $\approx$ 46 meV, fortunately in qualitative agreement with the recoilless TA, for which both energies would be 65 meV. (*Qualitative considerations* lead us to believe that a better calculation of the Debye-Waller factor would yield a fraction somewhat larger than the 10% fraction quoted above.)

We conclude our discussion of Ar on Cu by examining other properties of the outgoing distribution. From Table III, we see that the angular distribution is quite narrow (a half-width of 2^o), so that a detector with a wide aperture (about 8^o) could count all scattered particles simultaneously. We can also show that the scattered distribution is insensitive to the angle of incidence, so the experiment could be performed with the convenient total scattering angle of 90^o. Lastly, the temperature dependence of the no-loss peak of Fig. 5 is given in Fig. 6. As noted in section III, it is a gaussian near $T = 0$, but becomes an exponential for higher temperatures. The figure shows that the surface needs to be cooled to a temperature $T \lesssim 30K$ to ensure that the elastic peak is measurable.

We have also examined the possibility of using other heavy noble gases as incident

atoms. Clearly, for Kr or Xe, the scattering is closer to adiabatic than for Ar. However, the larger well-depths which these incident atoms experience reduces the Debye-Waller factor so much that the no-loss line is very small. We have also examined different crystals, to see if a larger Debye-Waller factor is likely to be found. In Table IV, we give results for three other surfaces : Ag, Al and Au. The potentials and surface elastic properties for these surfaces were estimated in the same way as those of Cu. Although the well-depth for Ag is very close to that of Cu, the increase in α, due to the lower Debye temperature, reduces its Debye-Waller factor . In the case of Al, it is the increased well-depth that leads to the reduction in the small Debye-Waller factor , while for Au, both these effects occur. However any of these surfaces are possible candidates for seeing this effect. On the other hand, the well-depth for Ar on W is so large[18] ($\sim$ 100 meV) that it is an unpromising choice.

V. Conclusions

A heavy incident atom, with fixed (thermal) energy scatters almost adiabatically from a target surface. For $T = 0$, in the limit of infinite mass, the Debye-Waller factor tends to a finite limit (< 1). This is because the slowly moving incident atom can only excite low frequency phonons. We used the trajectory approximation to estimate the final energy spectrum. We find that 20 meV Ar striking a cold ($T \leq 30$K) Cu(111) surface should exhibit substantial (about 10%) purely elastic scattering. Other rare gas/metal systems appear to be less favorable. This Debye-Waller factor becomes negligible at $T \approx 100$ K.

We have also shown in Appendix C that, for quasi-adiabatic weakly inelastic scattering, the trajectory approximation is valid. The question of its validity for strongly inelastic scattering and for the scattering of light atoms will form the subject of future work.

Although we used several simplifying assumptions we stongly believe that our basic

conclusion, that in the adiabatic limit ($m \to \infty$) the zero temperature Debye-Waller factor tends to a finite value, is independent of these.

Acknowledgements

We are very grateful to Jens Jensen, Horia Metiu and David Langreth for helpful conversations. This work has been supported by NSF grant DMR87-03434 and ONR grant N00014-89-J-1530 at Santa Barbara, and by NSF Grant DMR88-01027 at Rutgers. One of us (K.B.) also thanks the New Jersey Commission on Science and Technology for a Supercomputer Fellowship which provided partial support for this work.

Appendices

A. The Surface-Averaged Transfer Function.

In this appendix, we derive general expressions for the surfaced-averaged transfer function for a given atom-surface interaction. We restrict ourselves to potentials which may be written as a sum of pair potentials, and whose static corrugation is relatively small. We also consider only monatomic surfaces. We find the perpendicular component is a constant, independent of the interaction, and the parallel components vanish.

For a many-body interaction which is the sum of pair potentials, we may write

$$\sum_{\mathbf{l}} v(|\mathbf{r} - \mathbf{r_l} - \mathbf{u_l}|) \simeq \mathrm{V}_\perp(z - Z(\mathbf{R}, \{\mathbf{u}\})) \tag{A.1}$$

where $\mathrm{V}_\perp(z - Z(\mathbf{R}, \{\mathbf{u}\}))$ is the perpendicular potential approximating the true potential and $v(r)$ is the interaction between the incident atom and a single surface atom, a distance r apart. The label $\mathbf{l}$ ranges over all equilibrium positions $\mathbf{r_l}$ in the crystal, while $\mathbf{u_l}$ are the displacements of the crystal atoms from these positions. Now consider an infinitesimal displacement $\mathbf{u}$ of the $\mathbf{l} = 0$ atom (on the surface). Then

$$\mathrm{V}_\perp(z - Z_0(\mathbf{R}) - \mathbf{u}.\mathbf{f}(\mathbf{R})) = \sum_{\mathbf{l}} v(|\mathbf{r} - \mathbf{r_l} - \delta_{\mathbf{l},0}.\mathbf{u}|) \tag{A.2}$$

where $\mathbf{f}(\mathbf{R})$ is the transfer function (defined in the main text, equation (7)). Expanding the potential functions about their equilibrium values, we find

$$\mathbf{f}(\mathbf{R}) = \frac{v'(r)}{\mathrm{V}'_\perp(z - Z_0(\mathbf{R}))}\hat{\mathbf{r}} \tag{A.3}$$

where $\hat{\mathbf{r}} = \mathbf{r}/r$. The primes on the potentials indicate the derivatives with respect to their explicit dependent variable , i.e. $v'(r) = \mathrm{d}v/\mathrm{d}r, \mathrm{V}'_\perp(z - Z_0(\mathbf{R})) = \partial V_\perp/\partial z$. Note that, despite appearances, $\mathbf{f}(\mathbf{R})$ is implicitly independent of z, by definition. Then

$$\bar{\mathbf{f}}(0) = \frac{1}{\mathcal{A}}\int_S \mathrm{d}^2R \frac{v'(r)}{\mathrm{V}'_\perp(z - Z_0(\mathbf{R}))}\hat{\mathbf{r}} \tag{A.4}$$

Now we make use of our second assumption, viz. that $Z_0(\mathbf{R})$ is fairly smooth, to replace $V'_\perp(z - Z_0(\mathbf{R}))$ in the above expression by its average and to bring it outside the integral

$$\tilde{\mathbf{f}}(0) = \frac{1}{\mathcal{A}\overline{V'_\perp}} \int_S \mathrm{d}^2 R v'(r)\hat{\mathbf{r}} \tag{A.5}$$

where

$$\overline{V'_\perp} = \frac{1}{\mathcal{A}} \int_{\mathcal{A}} \mathrm{d}^2 R V'_\perp(z - Z_0(\mathbf{R})) \tag{A.6}$$

the average being taken over only one unit cell as the static potential has the translational symmetry of the surface . From equation (A.4) we see from symmetry that the transverse component,

$$\tilde{\mathbf{F}}(0) \equiv 0. \tag{A.7}$$

To find $\tilde{f}_3(0)$, we note from equation (A.6)

$$\overline{V'_\perp} = \frac{1}{\mathcal{A}} \int_{\mathcal{A}} \mathrm{d}^2 R \frac{\partial}{\partial z} \sum_{\mathbf{l}} v(|\mathbf{r} - \mathbf{r_l}|) \tag{A.8}$$

using equation (A.2) with $\mathbf{u} = 0$. By replacing $|\mathbf{r} - \mathbf{r_l}|$ with a new variable r in each sum we find

$$\overline{V'_\perp} = \frac{z}{\mathcal{A}} \int_S \mathrm{d}^2 R \frac{v'(r)}{r} \tag{A.9}$$

which, when substituted into equation (A.5), yields

$$\tilde{f}_3(0) = 1 \tag{A.10}$$

the desired result.

B. The surface displacement partial spectral density perpendicular to the surface for an isotropic elastic medium.

Near the adiabatic limit the incident atom excites only the low frequency phonons of the crystal, so we use only the long wavelength properties of the crystal. We estimate th-

desired quantities by treating the crystal as isotropic, which considerably simplifies the calculations.

The properties of an isotropic elastic medium with a surface (at $z = 0$) were originally calculated by Maradudin and Mills.[19] We define $\mathbf{v}_q$ to be an eigenvector of the dynamical matrix of the (half-)crystal, with normalization

$$\frac{1}{N}\sum_{\mathbf{l}} \mathbf{v}_q^*(\mathbf{l})\mathbf{v}_{q'}(\mathbf{l}) = \delta_{q,q'}, \tag{B.1}$$

where $\mathbf{l}$ labels the equilibrium positions of the atoms in the crystal, and N is the number of atoms in the crystal. As the crystal has translational symmetry parallel to the surface, we may write

$$\mathbf{v}_q(\mathbf{l}) = \mathbf{v}_q(l_3)e^{i\mathbf{Q}\cdot\mathbf{L}}. \tag{B.2}$$

For bulk phonons far within the crystal ($l_3 \to \infty$), $\mathbf{v}_q(l_3) = \hat{\mathbf{e}}_q e^{iq_3 l_3}$, where $\hat{\mathbf{e}}_q$ is a polarization vector of unit length. For bulk phonons at the surface of the crystal ($l_3 = 0$), the lengths of these vectors are greater than 1, due to enhancement of atomic displacements at the surface. Finally, for surface phonons, it should be noted that, for low frequency displacements, as $\omega \to 0$, the displacement vectors grow as $\omega^{1/2}$ (for bulk phonons, they are independent of ω). In terms of these displacement vectors, we may now define the Green's function by

$$d_{\alpha\beta}(\mathbf{Q}, l_3, l_3'; \omega^2) = \sum_q \frac{(\mathbf{v}_q^*(l_3))_\alpha (\mathbf{v}_q(l_3'))_\beta}{\omega^2 - \omega_q^2}, \tag{B.3}$$

which has been Fourier transformed parallel to the surface. Here α and β denote the Cartesian components. Then the displacement partial spectral density perpendicular to the surface is defined as

$$g(l_3;\omega) = \frac{1}{3N}\sum_q |(\mathbf{v}_q(l_3))_3|^2 \delta(\omega - \omega_q) \tag{B.4}$$

yielding

$$g(l_3;\omega) = \frac{S}{N}\int_0^{K_D} \frac{d^2Q}{(2\pi)^2}\frac{2\omega}{\pi}\mathrm{Im}d_{33}(Q, l_3, l_3; \omega^2 - i\epsilon) \tag{B.5}$$

where K_D is the two-dimensional Debye wavenumber, defined by

$$\pi K_D^2 = \left(\frac{2\pi}{\ell}\right)^2 \tag{B.6}$$

and ℓ ($\equiv 1/n^{1/3}$) is a measure of the atomic spacing. Because we have an elastic continuum, we may write

$$\mathrm{Im} d_{33}(Q, l_3, l_3; \omega^2 - i\epsilon) = Q c_t^2 \rho(l_3; \omega/Q c_t) \tag{B.7}$$

where ρ is a dimensionless function, given (for $l_3 = 0$) in equation (A6) of the appendix of Stutki and Brenig,[20] and c_t is the transverse velocity of sound in the bulk. Substituting this expression back into equation (B.5), and using the definition of K_D given in equation (B.6) and the standard Debye frequency, we find

$$g(l_3; \omega) = \frac{\gamma(l_3; \omega)\omega^2}{\omega_D^3} \Theta(\omega_D - \omega) \tag{B.8}$$

where

$$\gamma(l_3 = 0; \omega) = \frac{6}{2 + \sigma^3}[G_s^{(0)}(\infty) - G_s^{(0)}(\omega/Q c_t)] \tag{B.9}$$

and

$$G_s^{(n)}(x) = \int_0^x \frac{\rho(l_3 = 0; x')}{x'^{2+2n}} dx' \tag{B.10}$$

Here $\sigma = c_t/c_l$ is the ratio of transverse and longitudinal velocities in the bulk. Furthermore, as the Rayleigh velocity is the minimum velocity for any elastic wave in the surface, $G(x) = 0$ for $x \leq c_R/c_t$, where c_R is the Rayleigh wave velocity. Thus for low frequencies $\gamma(l_3; \omega) = \gamma(l_3)$ is a constant. From equation (B.8) it is clear that $\gamma(l_3) \to 1$ as $l_3 \to \infty$ (the interior of the crystal), while $\gamma_s \equiv \gamma(l_3 = 0)$ is generally larger than one, due to enhancement of atomic displacements at the surface. Furthermore we write $< u_3^2 >_s = \gamma_s/(4M\omega_D)$ as a measure of the mean-square displacement perpendicular to the surface at the surface (M is the mass of a surface atom). These definitions, and the spectral density of equation (B.8), lead to the simple form of equations (22) and (23) of the main text.

The result that $g_s(\omega)$ is proportional to ω^2 for small ω clearly depends only on the three-dimensional nature of the crystal. It is only in estimating the proportionality constant that we use the isotropic model as an approximation. For anisotropic crystals, we write $\sigma = \bar{c}_t/\bar{c}_l$, where the velocities have been averaged over all directions in the bulk.[21]

We conclude by noting that the factor μ occuring in equation (30) of the text, and contributing to the width of the angular distribution, is simply $G^{(1)}(\infty)/G^{(0)}(\infty)$.

C. Validity of the Trajectory Approximation in the Quasi-Adiabatic Regime

In this appendix we show that, for weakly inelastic scattering and small displacements of the surface atoms, the recoilless TA is valid in the quasi-adiabatic regime, i.e. when the mass of the scattered particle becomes large. This is because the incident atom does indeed behave classically, although the surface does not. We calculate the angle-integrated energy loss spectrum using the distorted wave Born approximation , and compare results with those found from equation (21).

In the language of quantum mechanical scattering theory we write, for the energy loss spectrum,[22]

$$\mathcal{N}(\epsilon) = \sum_{\mathbf{K}'} \frac{m^2}{k_3 k_3'} \sum_{\alpha} | < \alpha | T_{\mathbf{k}' \leftarrow \mathbf{k}} | 0 > |^2 \delta(E_\alpha - E_0 - \epsilon) \qquad \text{(C.1)}$$

where $T_{\mathbf{k}' \leftarrow \mathbf{k}}$ is the T matrix for scattering the incident atom with wavevector $\mathbf{k}$ to final wavevector $\mathbf{k}'$, with energy loss ϵ. It is an operator on the states $|\alpha>$ of the undisturbed crystal, where $|0>$ is the ground state. These states have energy E_α. To find this matrix element, we linearize the potential in the displacements of the surface atoms (see equation (6)) and, for weakly inelastic scattering, apply the first order distorted wave Born approximation:[22]

$$< \alpha | T^{(1)}_{\mathbf{k}' \leftarrow \mathbf{k}} | 0 > = \sum_{q} < \Psi_{k_3'} | F_\perp(z) | \Psi_{k_3} > \delta_{\mathbf{K}', \mathbf{K}+\mathbf{Q}} u_q(\omega_q), \qquad \text{(C.2)}$$

where $T^{(1)}$ is the leading inelastic contribution to the T matrix. Here $\Psi_{k_3}(z)$ is the scattering solution for an incident atom of perpendicular wavevector component k_3 scattered from $V_0(z)$. We have again used $\tilde{\mathbf{f}}(\mathbf{G}+\mathbf{Q}) = (0, \delta_{\mathbf{G},0})$ for simplicity.[23]

The delta functions in equations (C.1) and (C.2) impose conservation of energy and surface crystal momentum on the outgoing states. At fixed incident energy, as $m \to \infty$, both k_3 and $k_3' \to \infty$, so that WKB wavefunctions [24] may be used to calculate the matrix element containing $F_\perp(z)$. We write

$$< \Psi_{k_3'}|F_\perp(z)|\Psi_{k_3} >= \int_{-\infty}^{z_o} \mathrm{d}z \Psi^*_{k_3'}(z) F_\perp(z) \Psi_{k_3}(z) + \int_{z_o}^{\infty} \mathrm{d}z \Psi^*_{k_3'}(z) F_\perp(z) \Psi_{k_3}(z). \quad \text{(C.3)}$$

Here, the origin of the z-axis is chosen at the classical turning point of the particle with energy E, while z_o is chosen such that $z_o \gg \lambda$, but also so that $z_o \to 0$ as $m \to \infty$ (in a fashion described below). Thus, to evaluate the second integral, we may use the WKB states. We define these by

$$\chi^{(\pm)}_{k_3}(z) = \sqrt{\frac{k_3}{k_3(z)}} \mathrm{e}^{\pm i\phi(z)} \quad \text{(C.4)}$$

where

$$\phi(z) = \int_{z_o}^{z} k_3(z')\mathrm{d}z' \quad \text{(C.5)}$$

and $k_3(z) = \sqrt{k_3^2 - 2mV_\perp(z)}$. Then the physical scattering wavefunctions may be written

$$\Psi_{k_3}(z) = A^{(+)}_{k_3} \chi^{(+)}_{k_3}(z) + A^{(-)}_{k_3} \chi^{(-)}_{k_3}(z) \quad \text{(C.6)}$$

The second integral appearing in equation (C.3) will have four contributions. Consider the first of these :

$$M^{(++)} = A^{(+)}_{k_3'} A^{(+)*}_{k_3} \int_{z_o}^{\infty} \mathrm{d}z F_\perp(z) \sqrt{\frac{k_3 k_3'}{k_3(z) k_3'(z)}} \exp\{i[\phi_{k_3}(z) - \phi_{k_3'}(z)]\} \quad \text{(C.7)}$$

We may expand $\Delta k_3(z)$ ($\equiv k_3(z) - k_3'(z)$) for large m, and find $\Delta k_3(z) = m\omega/k_3(z)$ to leading order in $m^{1/2}$. In this expression, the denominator never vanishes, as we have excluded the turning point from our integration interval. Next we consider the classical

trajectory $z_{cl}(t)$ associated with the static perpendicular potential. We define it as a time-symmetric function starting at $-\infty$, reaching the turning point at $t = 0$ and continuing on to $+\infty$. On the interval 0 to ∞, it is an invertible function of t, so that $t = t_{cl}(z)$ is well-defined. Changing variables from z to t using this function, we find a very simple result for the phase of our integral, viz.

$$\phi_{k_3}(z) - \phi_{k_3'}(z) = \omega(t_{cl}(z) - t_o) \tag{C.8}$$

where $t_o = t_{cl}(z_o)$. We use the same change of variables for the entire integral, and use $k_3 \simeq k_3'$ in all other functions to get the leading order contribution:

$$M^{(+-)} = |A_{k_3}^{(-)}|^2 v \int_{t_o}^{\infty} dt F_\perp[z_{cl}(t)] e^{i\omega(t-t_o)}, \tag{C.9}$$

where v is the initial velocity of the incident particle. Finally, as $m \to \infty$ and $\lambda \to 0$, so that $t_o \to 0$, the integrand is well-behaved and we have

$$M^{(++)} = |A_{k_3}^{(+)}|^2 v \frac{F_\perp(\omega)}{2} \tag{C.10}$$

where $F_\perp(\omega)$ is the Fourier transform of the classical force exerted on the incident atom. In an obvious notation, we find $M^{(+-)} = M^{(-+)} = 0$ due to the rapid oscillation of the phases in the integrals, while, from symmetry, $M^{(--)} = |A_{k_3}^{(-)}|^2 v F_\perp(\omega)/2$. Then, conservation requirements yield

$$< \Psi_{k_3'} | F_\perp(z) | \Psi_{k_3} > = v F_\perp(\omega). \tag{C.11}$$

Inserting this matrix element back into the T matrix, and using that to calculate the energy loss spectrum, we find identical results to the TA for weakly inelastic scattering (i.e. expanding the exponential in equation (18) in a power series, and keeping only the first term).

We conclude by showing that the first integral in equation (C.3) is negligible in the adiabatic limit. First note that, for $z \leq -z_o$, we may again use WKB to show that this

contribution becomes exponentially small as $m \to \infty$. Then, around the turning point $z = 0$, there is a small interval, $-d$ to d, in which the potential may be well-approximated by a linear function. The value of d depends only on E and the shape of the potential, and is therefore independent of m. For $-d < z < d$, we may use Airy functions to approximate the wavefunctions. If we choose $z_o = (2mF_{\_}(t = 0))^{-1/3}$, where $F_{\_}(0)$ is the classical force at the turning point, we find the integral from $-z_o$ to z_o to be finite, and proportional to z_o. This choice obeys the requirements stated above, and yields a vanishing contribution (of $O(m^{-1/3})$) as $m \to \infty$. This completes the proof.

References

*Present address: Department of Physics and Astronomy, Rugters University, P.O. Box 849, Piscataway, NJ 08855-0849.

1. G. Benedek, J. P. Toennies and R. B. Doak, Phys. Rev. B **28**, 7277 (1983).
2. A. Amirav, M. J. Cardillo, P. L. Trevor, Carmay Lim and J. C. Tully, J. Chem. Phys. **87**, 1796 (1987).
3. Carmay Lim, J. C. Tully, A. Amirav, P. L. Trevor and M. J. Cardillo, J. Chem. Phys. **87**, 1808 (1987).
4. E. K. Schweizer and C. T. Rettner, Phys. Rev. Lett. **62**, 3085 (1989).
5. Although one can imagine freak situations in which exactly no energy loss occurs classically, but these occurences are infinitely rare compared to those in which ΔE is finite.
6. V. Bortolani, V. Celli, A. Franchini, J. Iododi, G. Santoro, K. Kern, B. Poelsema and G. Comsa, Surf. Sci. **208**,1 (1989).
7. N. W. Ashcroft and N. D. Mermin, *Solid State Physics* (Holt, Rinehart and Wilson, Philadelphia, 1976), page 486.
8. As shown in Section III, surface modes do not alter the qualitative conclusions.
9. J. L. Beeby, J. Phys. C **4**, L359, (1971).
10. R. Brako and D. M. Newns, Surf. Sci. **117**, 42 (1982).
11. M. Born and K. Huang in *Dynamical Theory of Crystal Lattices*, Clarendon Press, 1968, page 402.
12. Our final results are independent of the exact choices of d and τ.
13. The precise value of d drops out of this expression.

14. R. Sedlmeir and W. Brenig, Z. Phys. B - Condensed Matter **36**, 245 (1979).

15. E. Zaremba and W. Kohn, Phys. Rev. B **15**, 1769 (1977).

16. N. Esbjerg and J. K. Norskov, Phys. Rev. Lett. **45** , 807 (1980).

17. M. W. Cole and F. Toigo, Phys. Rev. B **31**, 727 (1985).

18. J. Böheim and W. Brenig, Z. Phys. B - Condensed Matter **41**, 243 (1981).

19. A. A. Maradudin and D. L. Mills, Ann. Phys. **100**, 262 (1976).

20. J. Stutki and W. Brenig, Z. Phys. B - Condensed Matter **45**, 49 (1981).

21. *CRC Handbook of Chemistry and Physics*, 70th edition, ed. R. C. Weast, CRC Press Inc., 1989, page E-44.

22. V. Bortolani and A. C. Levi , Rivista del Nuovo Cimento **9** 1 (1986).

23. For this argument, we need only that $\tilde{\mathbf{f}}(\mathbf{K}) \rightarrow 0$ as $K \rightarrow 0$.

24. See, for example, M. V. Berry and K. E. Mount, Rep. Prog. Phys. **35**, 315 (1972).

Table Captions

(I) Constants characterizing quasi-adiabatic scattering for three different potentials: the exponential repulsion, the Morse potential and the potential used to model the Ar/Cu system.

(II) Properties of Cu surface and Ar-Cu interaction used to calculate Fig. 5. The sources are given in the main text. The potential parameters should not be regarded as highly accurate.

(III) Calculated properties of quasi-adiabatic scattering for the energy loss spectrum of Fig. 5.

(IV) Calculated Debye-Waller factors for Ar on three different crystals. D denotes the estimated well-depth and α is defined by equation (23).

constant	exponential	Morse	Ar/Cu
I_0	2.07	25.1	21.7
I_1	0.72	31.0	23.0
I_2	0.41	52.5	34.4
I_3	0.31	111	64.9
e^{-2W}	0.93	0.04	0.10
$\bar{n}$	0.07	3.1	2.3

Table I

parameter	symbol	value
strength of repulsion	A_o	85.7 eV
repulsive decay length	d	0.37Å
Van der Waals constant	C_3	1.50 eV Å^3
position of reference plane	z_{ref}	0.259 Å
depth of attractive well	D	45.4 meV
surface phonon enhancement	γ	1.8

Table II

variable	value
$\bar{\omega}$	8.2 meV
$\overline{\Delta E}$	19 meV
T_τ	63 K
$\bar{T}$	19 K
$\tilde{T}$	14 K
θ_W	2^o
$\bar{\omega}/\omega_D$	0.30

Table III

metal	$D(\mathrm{meV})$	$\alpha/\alpha_{\mathrm{Cu}}$	$e^{-2W}(\%)$
Ag	44.6	1.60	3.2
Al	64.5	1.18	1.1
Au	69.6	2.17	0.09

Table IV

Figure Captions

(1) Typical (angle-integrated) energy loss spectrum for atom-scattering from a cold surface. The no-loss line has been broadened to simulate finite energy resolution.

(2) Change in energy loss spectrum for a heavy particle when incident mass is doubled. The inelastic shoulder grows in height (by a factor of $\sqrt{2}$) and is compressed towards $\Delta E = 0$ (again by a factor of $\sqrt{2}$), so that its total area remains unchanged. The no-loss peak does not change at all, so that the Debye-Waller factor remains finite.

(3) Schematic of corrugation function for a many-body potential. (a) The heavy lines indicate atomic positions and corrugation function at equilibrium positions. The dashed line shows the change in the corrugation function due to moving the central atom a small amount perpendicular to the surface. (b) The transfer function in the perpendicular direction.

(4) Fourier transform of classical accelerations for two potentials in dimensionless variables : $\nu = \omega\tau$ and $\zeta'' = \ddot{z}_\omega/v$.

(5) Energy loss spectra for two potentials in the quasi-adiabatic regime. Only weakly inelastic scattering occurs for the exponential ($\bar{n} = 0.07$), but for the Morse potential, the acceleration due to the well leads to strongly inelastic scattering ($\bar{n} = 3.1$).

(6) Calculated total final energy spectrum for 20 meV Ar striking Cu (111) at zero temperature. The scattering is about 10% elastic. An energy resolution of only 10% was assumed, and the no-loss peak is clearly visible.

(7) The dependence on surface temperature of the peak shown in Fig. 5.

Fig. 1 (Burke et al)

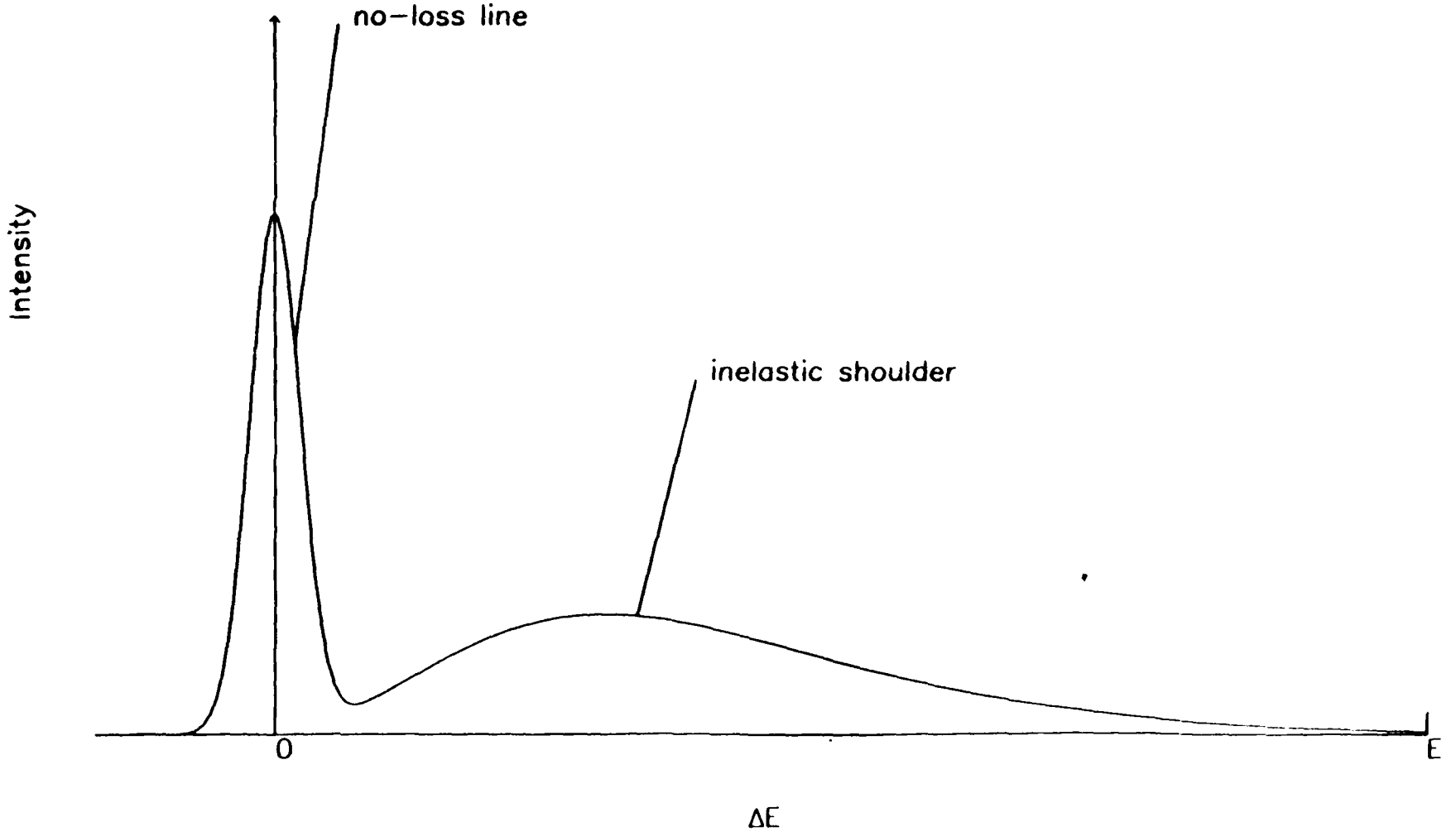

Fig. 2 (Burke et al)

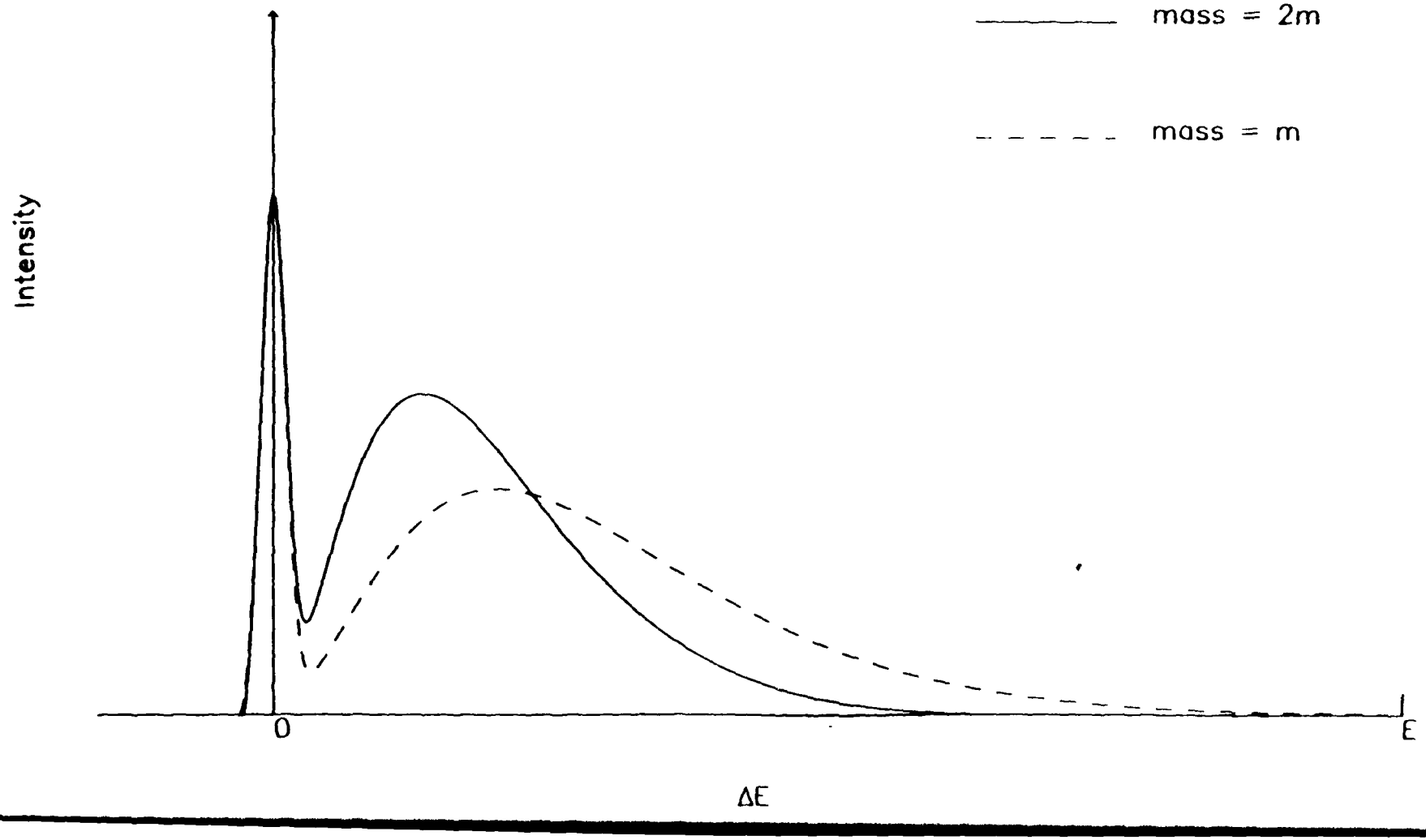

Fig. 3 (Burke et al)

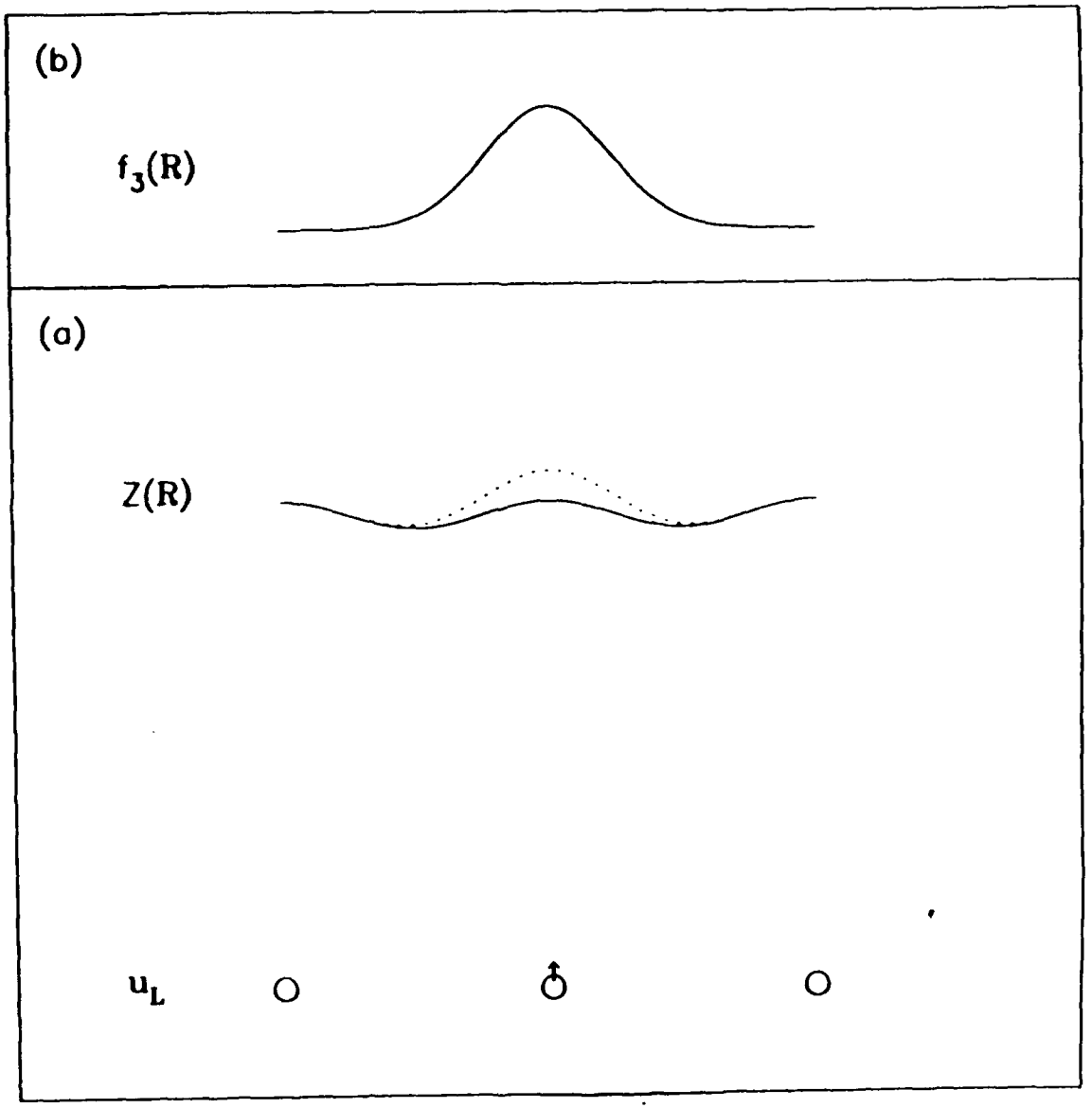

Fig. 4 (Burke et al)

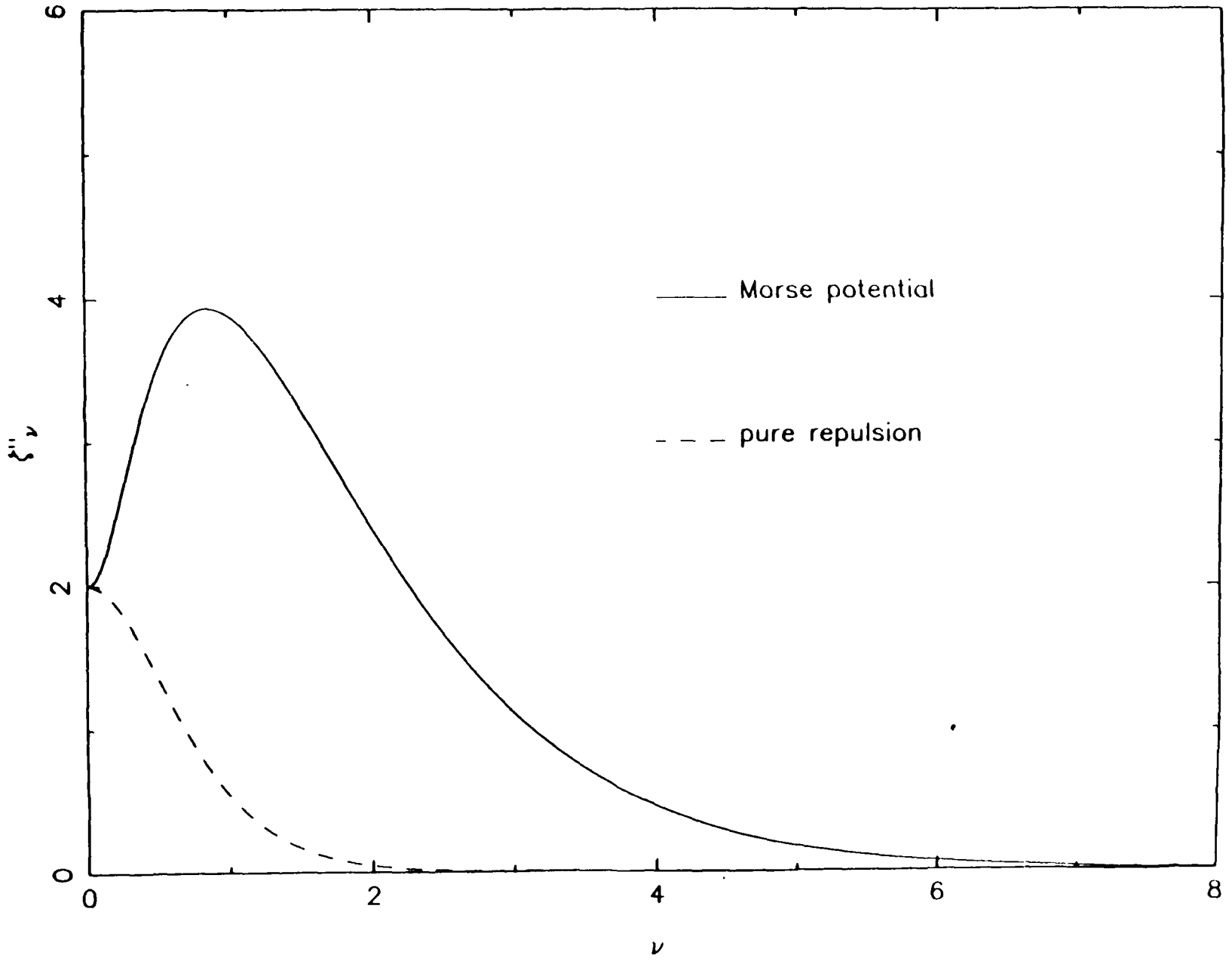

Fig. 5 (Burke et al)

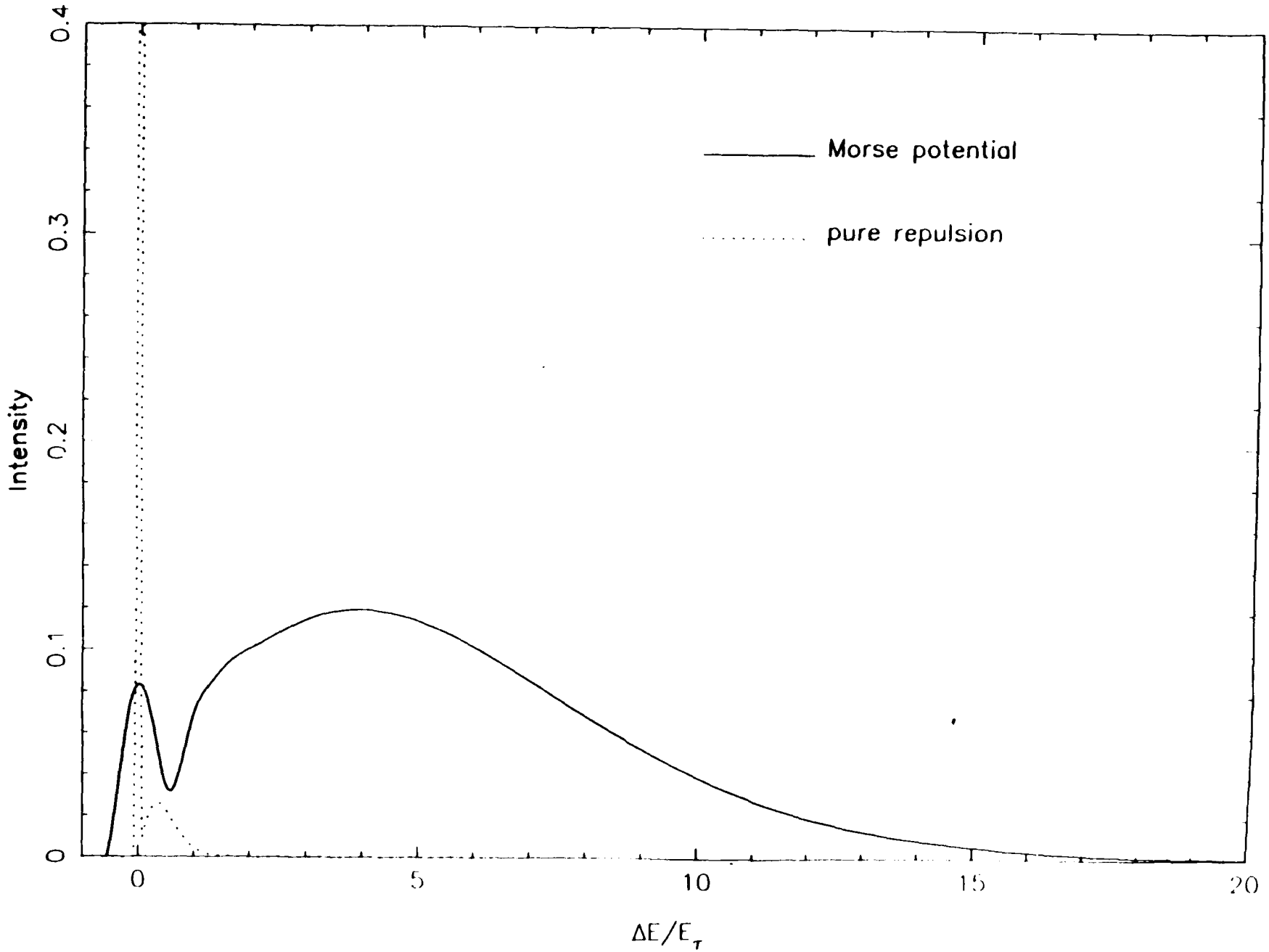

Fig. 6 (Burke et al)

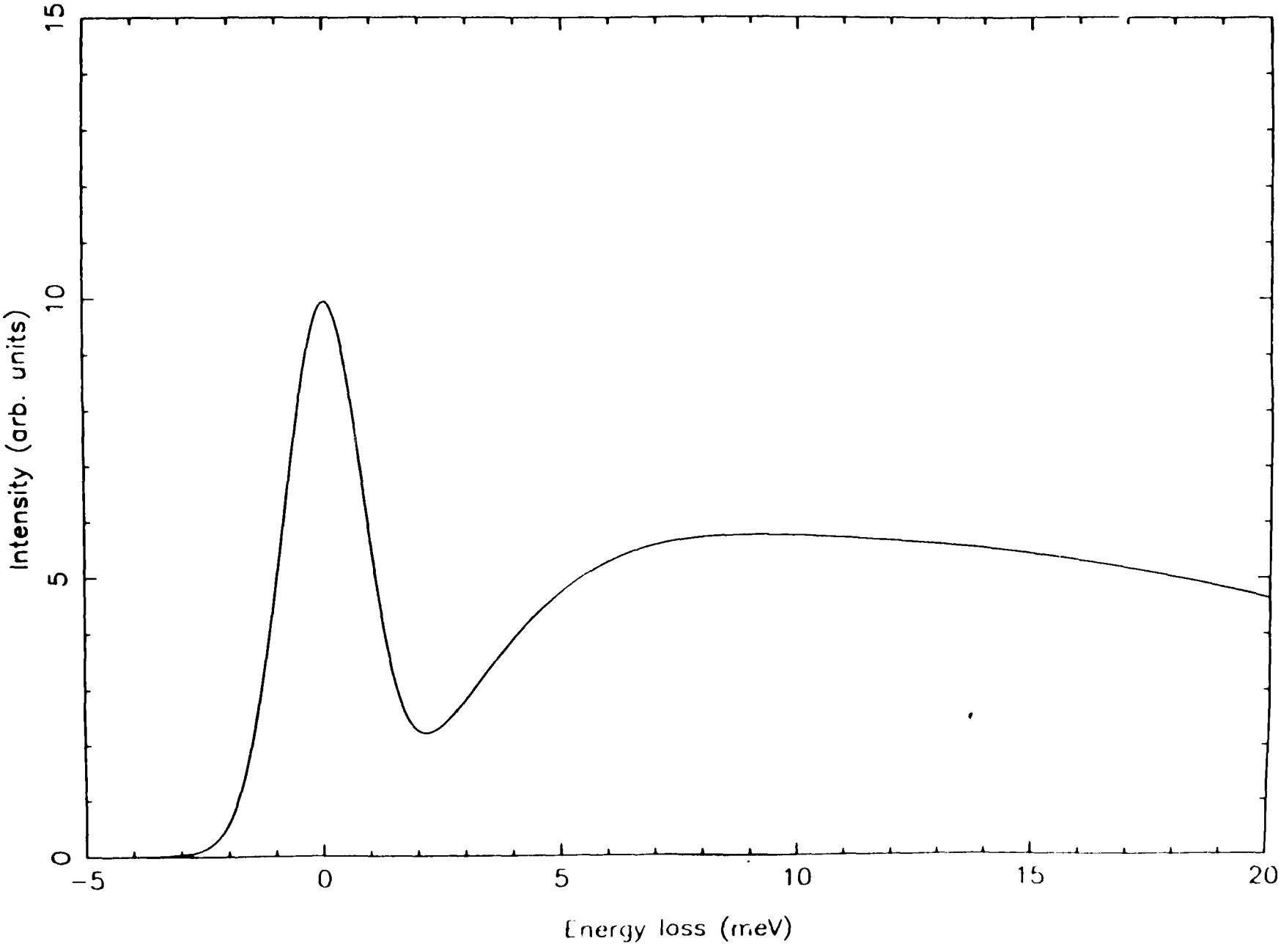

Fig. 7 (Burke etal)